

Exploration of two highly fluorinated ammonium cations as spacers in low- and mixed dimensional hybrid lead iodide perovskites

Concetta Bafaro,^a Sofia Girolmoni,^a Cesare Boriosi,^{a,b} Edoardo Mosconi,^b Marco Cavazzini,^b Simonetta Orlandi,^b Francesco Toniolo,^c Giulia Grancini,^c Mohammad Khaja Nazeeruddin,^d Ferdinando Costantino*^a and Gianluca Pozzi*^b

^a Department of Chemistry, Biology and Biotechnologies. University of Perugia, 06123 Perugia, Italy

^b CNR Institute of Chemical Sciences and Technologies "Giulio Natta" (CNR-SCITEC), 20133 Milan, Italy

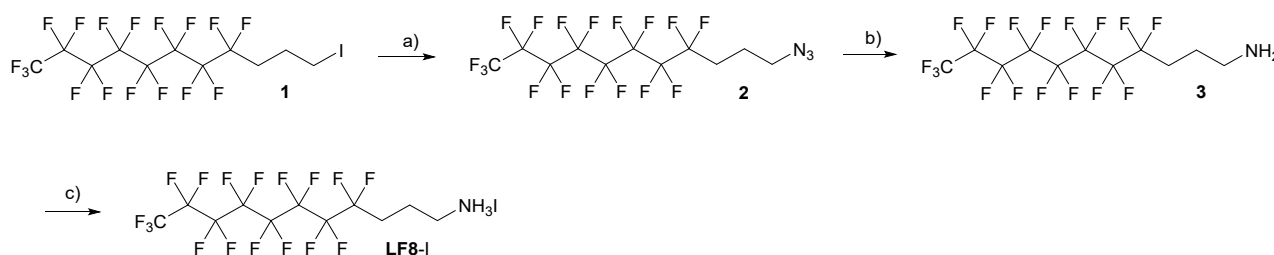
^c Department of Chemistry, University of Pavia, 27100 Pavia, Italy

^d School of Integrated Circuits, Southeast University, Wuxi, Jiangsu, 214026 P. R. China

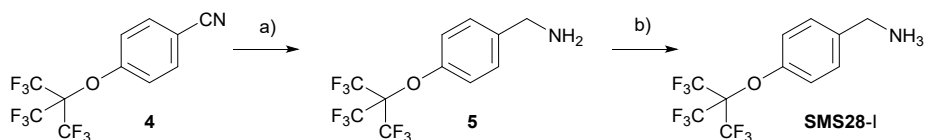
Electronic supplementary information

Synthesis of organic salts

The ammonium salts **LF8-I** and **SMS28-I** were prepared as summarized in **Schemes S1** and **S2**.



Scheme S1. a) NaN_3 , DMSO, 100 °C; b) $\text{Zn}/\text{NH}_4\text{Cl}$, EtOH, reflux; c) HI_{aq} 57%, MeOH, RT



Scheme S2. a) LAH, Et_2O , 0 °C to RT; b) HI_{aq} 57%, MeOH, RT.

Materials and methods. Commercially available chemicals and solvents were used without any further purification. 4,4,5,5,6,6,7,7,8,8,9,9,10,10,11,11,11-Heptafluoroundecan-1-amine **3** is a known compound.¹ It was prepared by us following a more convenient synthetic procedure for laboratory scale operations as here reported. Reactions were monitored by thin layer chromatography (TLC) that was conducted on plates precoated with silica gel Si 60-F254 (Merck, Germany). ^1H NMR, ^{13}C NMR, and ^{19}F NMR spectra were recorded on a Bruker Avance 400 spectrometer (400, 100.6, and 377 MHz, respectively). Chemical shifts are reported in ppm downfield from SiMe_4 , with the residual proton (CHCl_3 : $\delta=7.26$ ppm, DMSO: $\delta=2.50$ ppm) and carbon (CDCl_3 : $\delta=77.0$ ppm, DMSO- d_6 : $\delta=39.5$ ppm) solvent resonances as internal references. Chemical shifts for ^{19}F NMR spectra are reported in ppm relative to an external standard (CFCl_3 ,

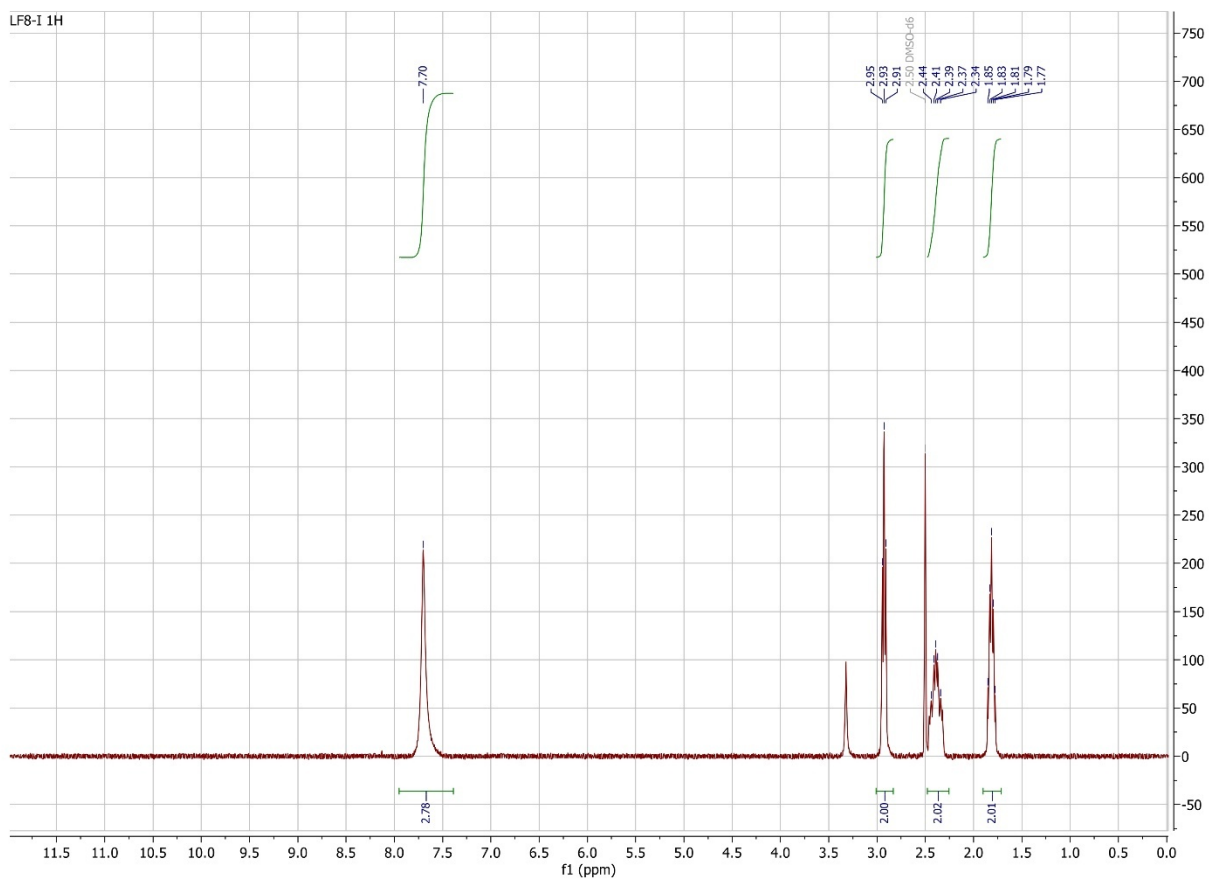
$\delta=0$). Elemental analyses were carried out by the Departmental Service of Microanalysis (University of Milano).

11-Azido-1,1,1,2,2,3,3,4,4,5,5,6,6,7,7,8,8-heptadecafluoroundecane (2). The title compound was prepared according to a slight modification of the procedure reported by Rábai and coworkers.² In a flame dried Schlenk tube equipped with a stir bar, NaN₃ (0.39 g, 6.0 mmol) and 1-iodo-4,4,5,5,6,6,7,7,8,8,9,9,10,10,11,11,11-heptadecafluoroundecane **1** (2.94 g, 5.0 mmol) were suspended in dry DMSO (10 mL) under nitrogen. The mixture was heated to 100 °C under stirring for 5 h, then stirring was stopped and the mixture was cooled to room temperature to give a liquid biphasic system. After separation, the upper layer was extracted twice with Et₂O (3 x 5 ml) and discarded. The ether extracts and the bottom layer were combined, washed with water (3x 10 ml), brine, and dried over MgSO₄. The solvent was removed by evaporation at 45 °C under atmospheric pressure, then at room temperature and 70 mbar for 10 minutes. The product (2.35 g, yield = 93%) was obtained as a colorless viscous oil. Physical and spectral data agreed with those reported in the literature.²

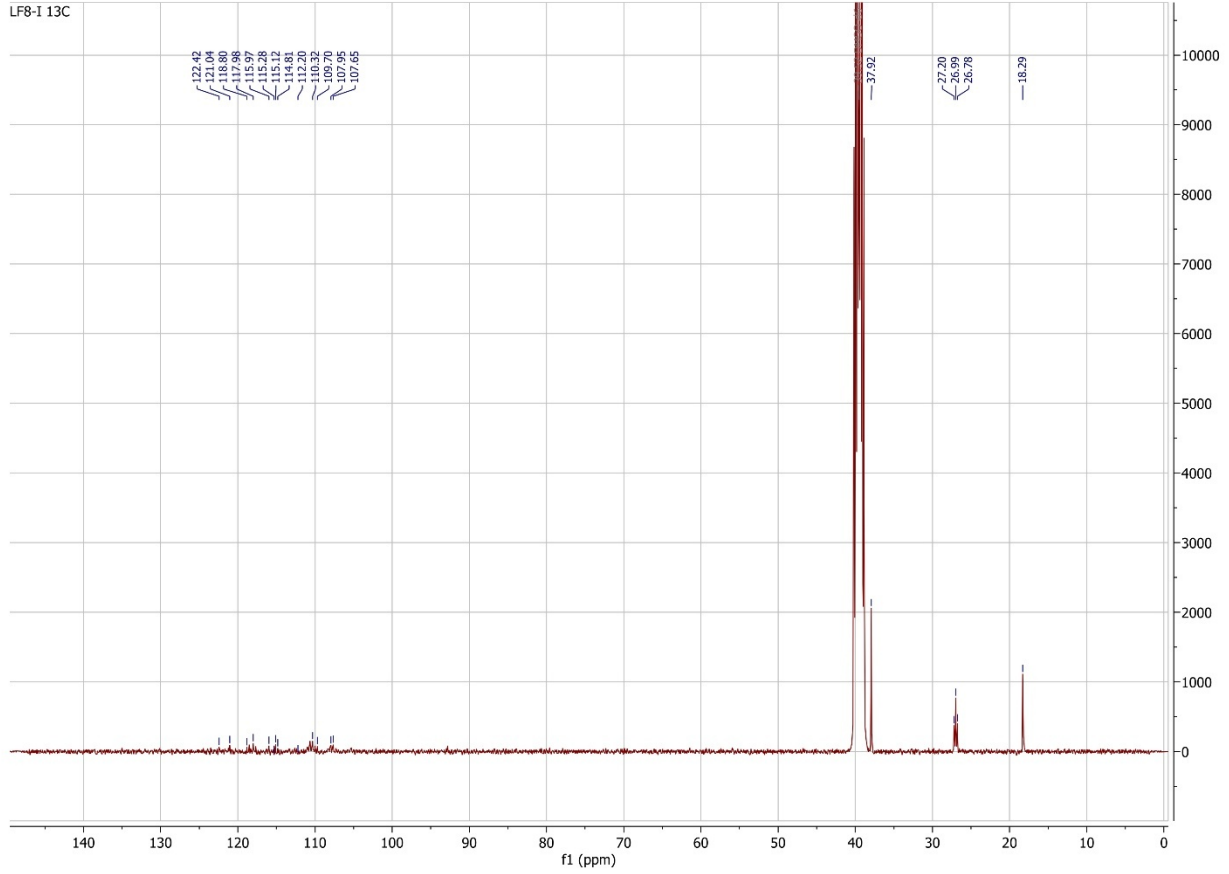
4,4,5,5,6,6,7,7,8,8,9,9,10,10,11,11,11-Heptadecafluoroundecan-1-amine (3). To a suspension of azide **2** (2.01 g, 4.0 mol) and ammonium chloride (0.50 g, 9.35 mol) in EtOH (10 mL) and water (3 mL), zinc powder (0.34 g, 5.2 mol) was added. The mixture was stirred vigorously at refluxing for 1 h, then it was cooled to room temperature. Et₂O (25 mL) and aqueous ammonia (2 mL) was added. The solid residue was filtered off and the liquid organic phase was separated, washed with water (3 x 5 ml), brine, and dried over MgSO₄. The solvent was removed by evaporation under reduced pressure, to give the product (1.70 g, yield = 89%) as a yellowish viscous oil. Physical and spectral data agreed with those reported in the literature.¹

4,4,5,5,6,6,7,7,8,8,9,9,10,10,11,11,11-Heptadecafluoroundecan-1-ammonium iodide (LF8-I). To a stirred suspension of amine **3** (1.43 g, 3.0 mmol) in MeOH (10 mL), aqueous HI 57% wt (0.42 mL, about 3.2 mmol) was added dropwise. The solution was stirred for 30 min, then the solvent was evaporated under reduced pressure, followed by addition of toluene (5 mL) and evaporation under reduced pressure. Addition/evaporation of toluene was repeated twice. The solid residue was thoroughly washed with AcOEt, dried in air and redissolved in a minimal amount of MeOH (about 5 mL). The solution was added dropwise to rapidly stirring Et₂O (70 mL), to give **SMS25-I** (0.90 g, yield = 66%) as a white fluffy precipitate that was recovered by filtration on a Büchner funnel. Mp = 241-242 °C. ¹H NMR (401 MHz, DMSO) δ 7.70 (br s, 3H), 2.93 (t, $J = 7.4$ Hz, 2H), 2.48–2.30 (m, 2H), 1.87–1.77 (m, 2H). ¹³C NMR (101 MHz, DMSO) δ 122.42–107.65 (m, -C₈F₁₇), 37.92, 26.99 (t, ²J_{CF} = 21.7 Hz, C), 18.29. ¹⁹F NMR (377 MHz, DMSO) δ -81.3 (t, ³J_{F,F} = 9.7 Hz, 3F), -

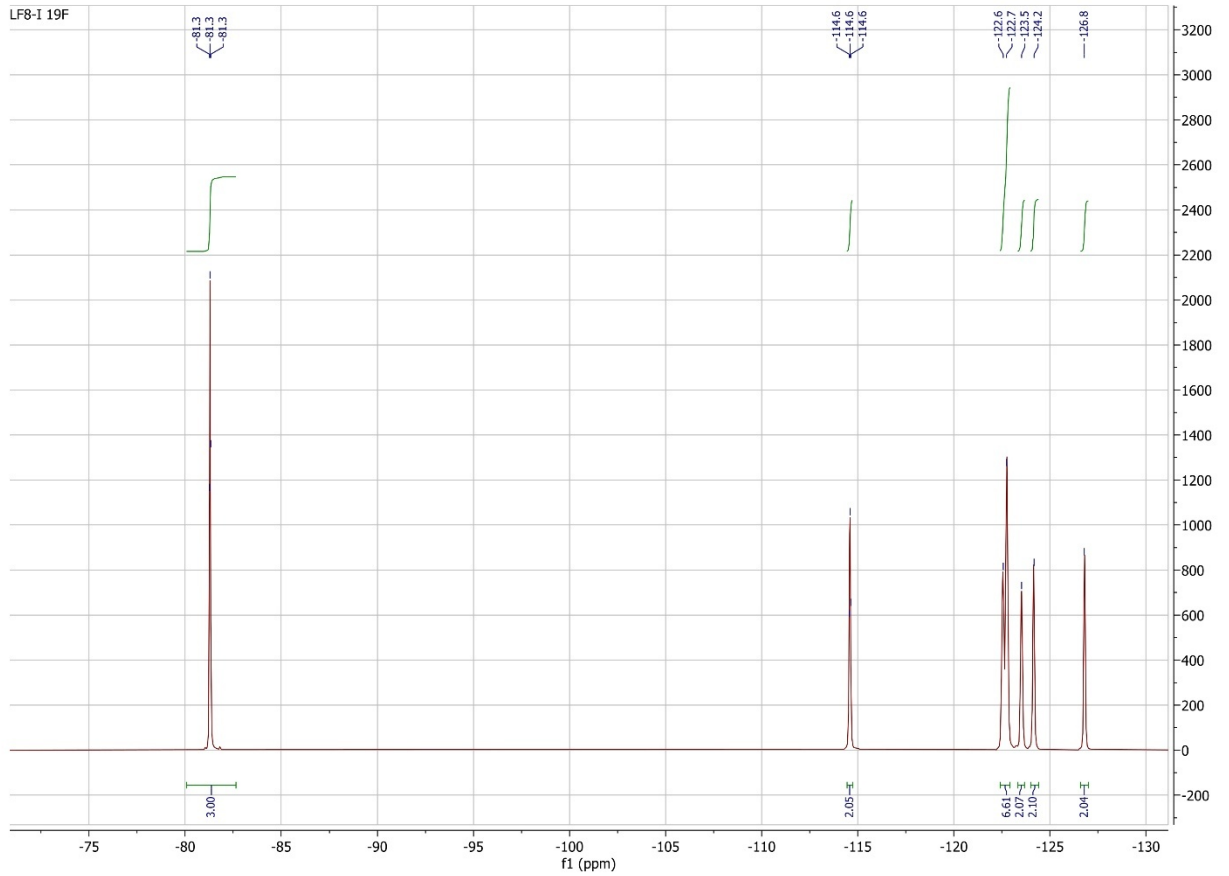
114.6 (t, $^3J_{F,F} = 14.2$ Hz, 2F), -122.6 (m, 6F), -123.5 (br s, 2F), -124.2 (br s, 2F), -126.8 (br s, 2F). Anal. Calcd for $C_{11}H_9F_{17}N$: C, 21.84; H, 1.50; N, 2.31. Found: C 21.81, H 1.54, N 2.26. NMR spectra are shown here below.



LF8-I 13C

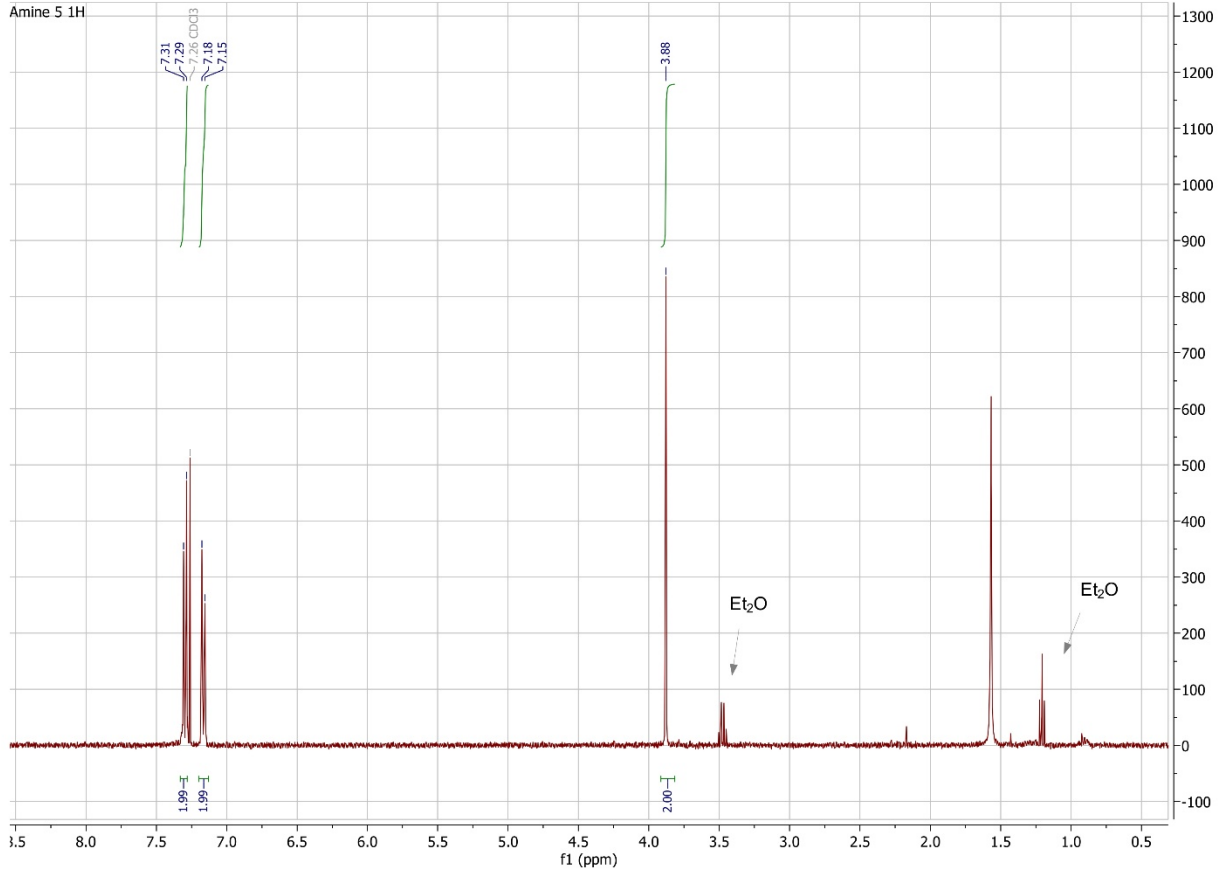


LF8-I 19F

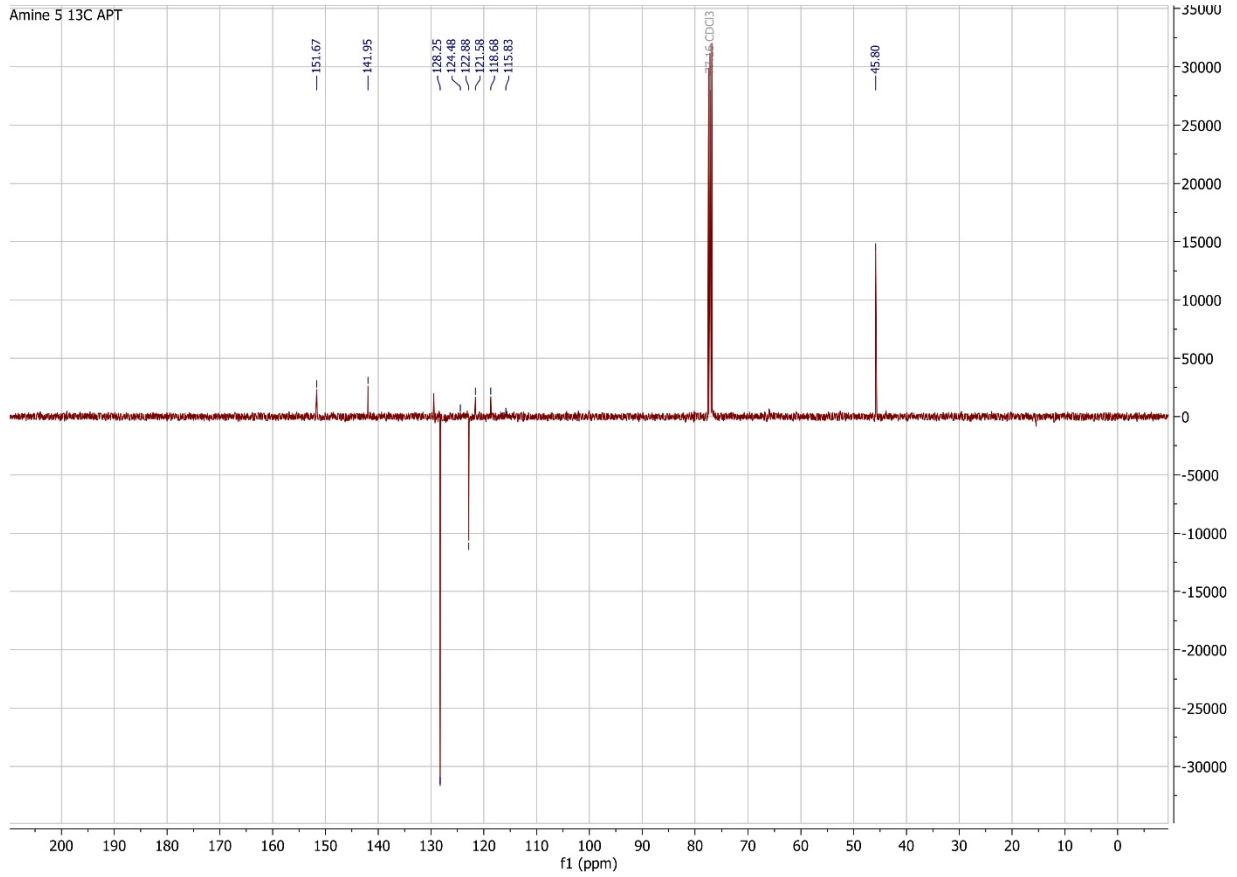


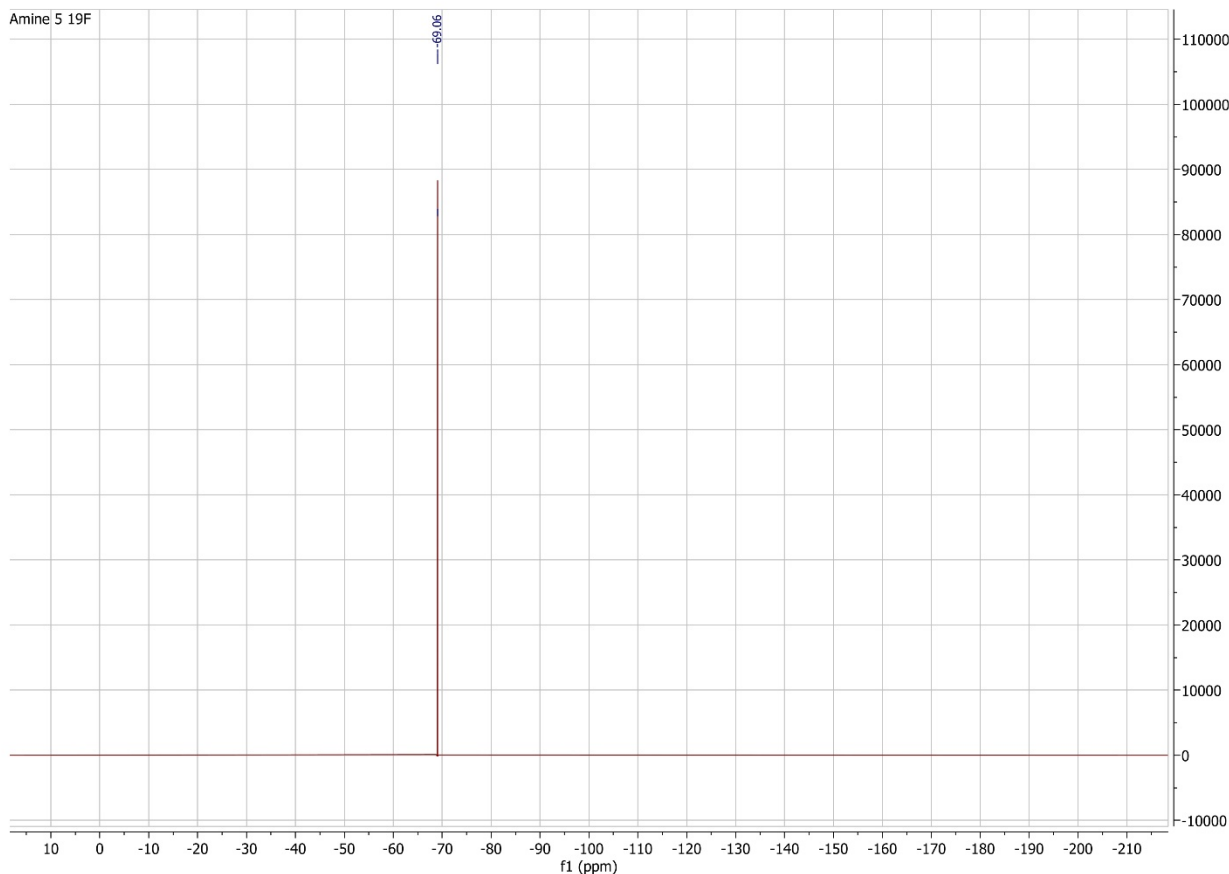
4-(Nonafluoro-*tert*-butoxy)benzylamine (5). In a flame-dried two-neck flask equipped with a stir bar, a condenser and a dropping funnel, LAH (0.46 g, 12.0 mmol) was suspended in dry Et₂O (20 mL). The flask was cooled to 0 °C, and then a solution of 4-(nonafluoro-*tert*-butoxy)benzotrile **4³** (2.02 g, 6.0 mmol) in dry Et₂O (10 mL) was added dropwise. The mixture was stirred at 0 °C for 15 min and then at room temperature for 3 h. The mixture was cooled to 0 °C and water (0.8 mL) was added dropwise, followed by 20% aqueous NaOH (0.6 mL), then another portion of water (2.8 mL). The solution was warmed to room temperature, stirred for an additional 15 min, and then filtered through Celite. The inorganic solid material was washed with Et₂O (2 x 10 mL). The filtrate and washing were combined. The organic phase was separated, washed with water (3 x 10 mL), brine, and dried over MgSO₄. The solvent was removed by evaporation under reduced pressure, to give the product (1.84 g, yield = 90%) as a yellowish oil containing traces of Et₂O that was used for the next step without further purification. ¹H NMR (400 MHz, CDCl₃) δ 7.30 (d, *J* = 8.9 Hz, 2H), 7.17 (d, *J* = 8.5 Hz, 2H), 3.88 (s, 2H). ¹³C NMR (101 MHz, CDCl₃) δ 151.67, 141.95, 128.24, 122.89, 120.13 (q, ¹*J*_{C,F} = 292 Hz, -CF₃), 45.80. ¹⁹F NMR (282 MHz, CDCl₃) δ = -69.07 (s, 9F). NMR spectra are shown here below.

Amine 5 1H



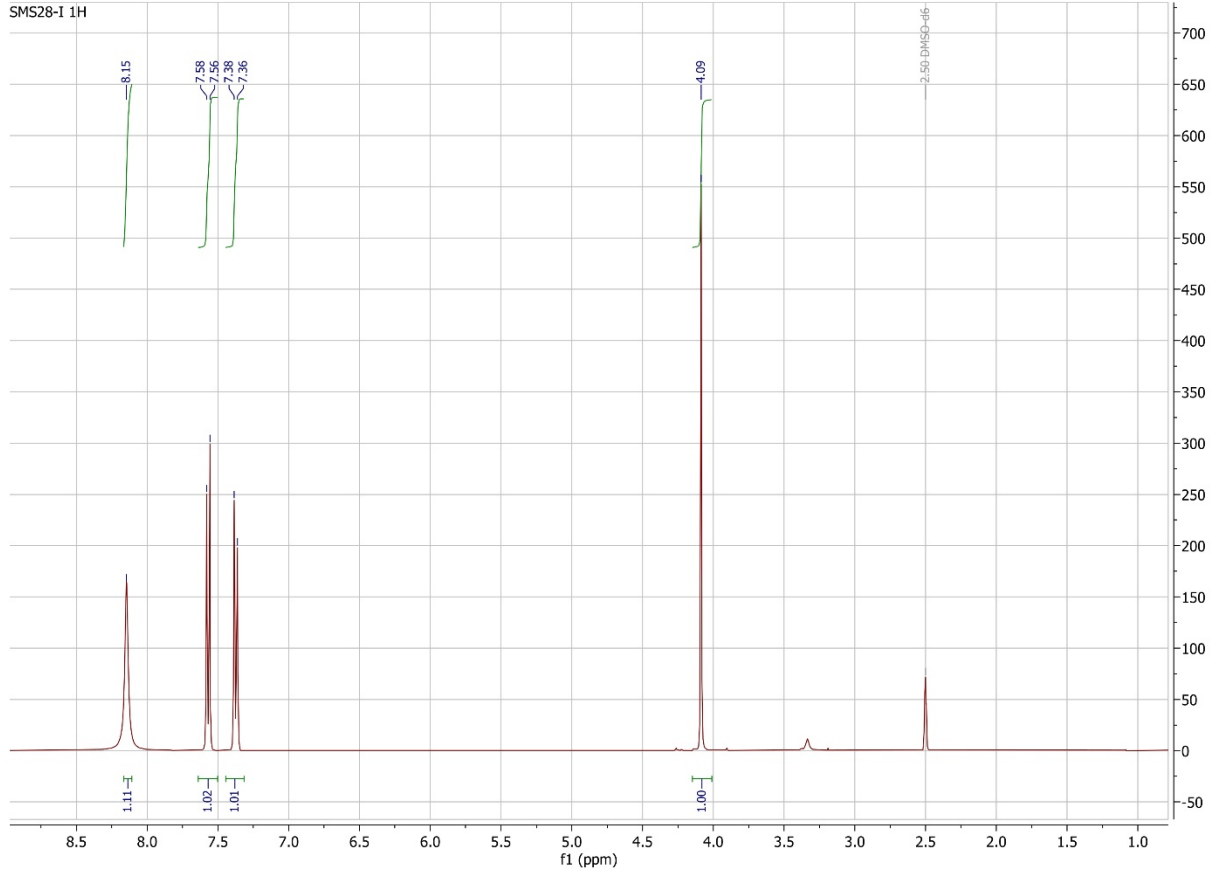
Amine 5 13C APT



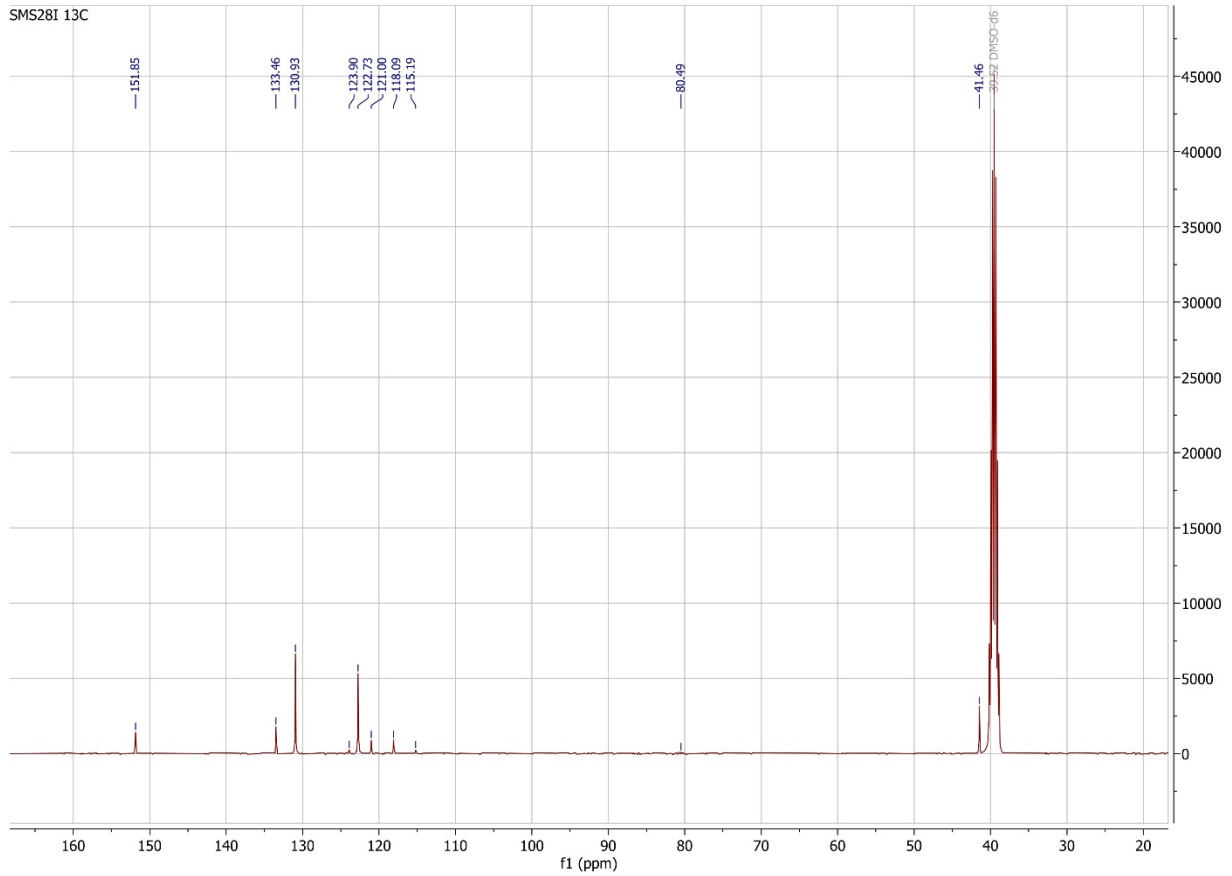


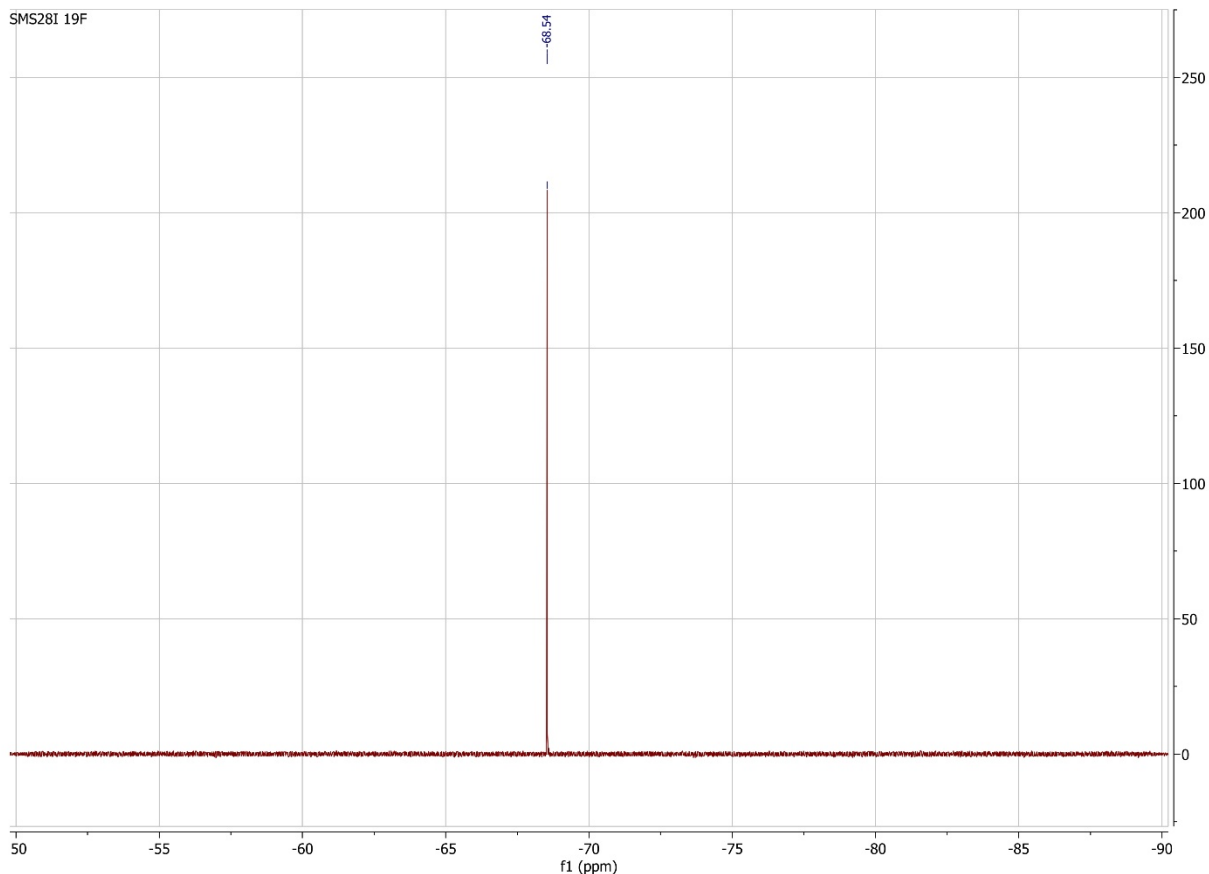
4-(Nonafluoro-*tert*-butoxy)benzylammonium iodide (SMS28-I). To a stirred solution of amine **5** (1.84 g, 5.4 mmol) in MeOH (20 mL), aqueous HI 57% wt (0.75 mL, about 5.5 mmol) was added dropwise. The solution was stirred for 30 min, then the solvent was evaporated under reduced pressure, followed by addition of toluene (5 mL) and evaporation under reduce pressure. Addition/evaporation of toluene was repeated twice. The solid residue was thoroughly washed with AcOEt, dried in air and redissolved in a minimal amount of MeOH (about 5 mL). The solution was added dropwise to rapidly stirring Et₂O (70 mL), to give **SMS25-I** (2.08 g, yield = 82%) as a white precipitate that was recovered by filtration on a Büchner funnel. Mp = 252 °C. ¹H NMR (400 MHz, DMSO-*d*₆) δ 8.12 (br s, 3H), 7.57 (d, *J* = 8.7 Hz, 2H), 7.37 (d, *J* = 8.5 Hz, 2H), 4.097 (s, 2H). ¹³C NMR (101 MHz, DMSO-*d*₆) δ 151.85, 133.46, 130.93, 122.73, 119.51 (q, ¹*J*_{CF} = 292, -CF₃), 80.49 (m, -C(CF₃)₃) 41.46. ¹⁹F NMR (377 MHz, DMSO-*d*₆) δ -68.54 (s, 9F). Anal. Calcd for C₁₁H₉F₉INO: C 28.17, H 1.93, N 2.99. Found: C 28.16, H 1.98, N 2.97. NMR spectra are shown here below.

SMS28-1 1H



SMS281 13C





Lead iodide (PbI₂) synthesis. Two aqueous solutions, both 500 ml, containing respectively 6.00 g (18mmol) of Pb(NO₃)₂ and 6.06 g (36,5 mmol) of KI were prepared. Once KI was rapidly added to the Pb(NO₃)₂ solution at room temperature, under stirring, the PbI₂ precipitate was instantly obtained. The resulting suspension was filtered by gravity and the product was recovered from the filter. The formation of PbI₂ was confirmed by X-Rays Powders Diffraction (XRPD, **Figure S1**).

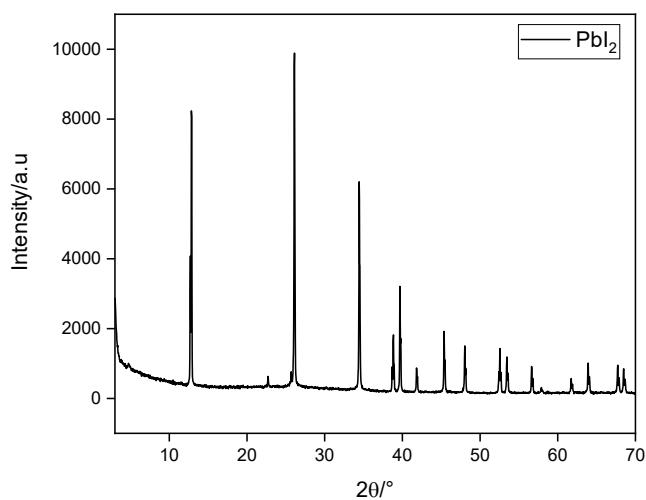


Figure S1. XRPD Pattern of the PbI₂ powder obtained from the synthesis.

$(\text{RNH}_3)_2\text{PbI}_4$ thin film optical characterization

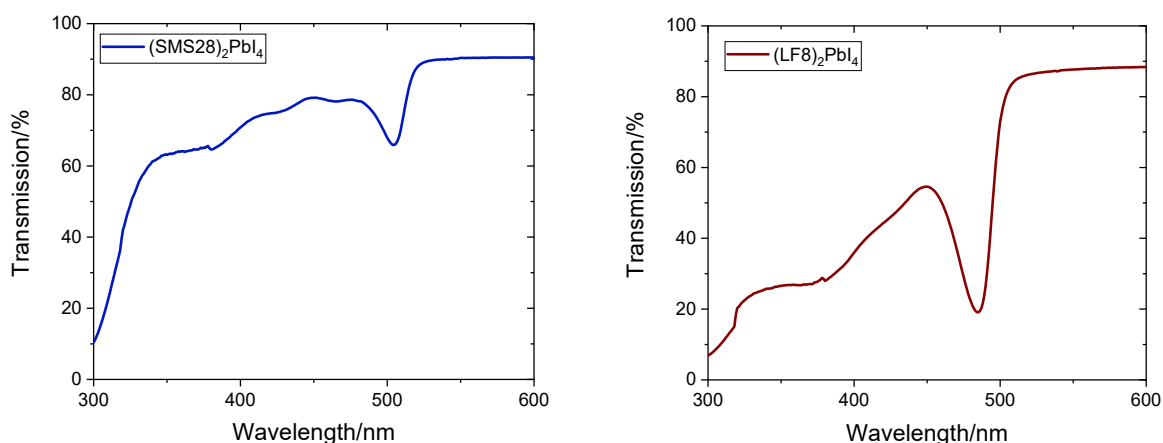


Figure S2. Transmission UV-Vis spectra of $(\text{SMS28})_2\text{PbI}_4$ (left) and $(\text{LF8})_2\text{PbI}_4$ (right) thin films.

$(\text{RNH}_3)_2\text{PbI}_4$ powders synthesis and structural characterization

2D perovskite powders were obtained by slow evaporation at 70°C of 0.75 mL of a DMSO solution containing the fluorinated ammonium salt **LF8-I** or **SMS28-I** (1.15 M) and PbI_2 (0.57 M) in a 2:1 molar ratio. The materials formation was confirmed by XRPD patterns (**Figure S3**).

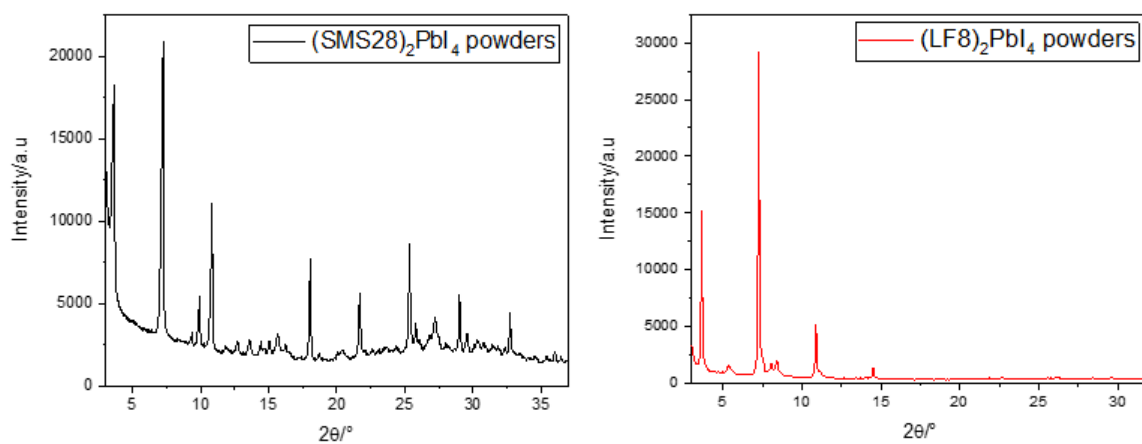


Figure S3. XRPD patterns of $(\text{SMS28})_2\text{PbI}_4$ (left) and $(\text{LF8})_2\text{PbI}_4$ (right) powders.

XRPD of $(\text{SMS28})_2\text{PbI}_4$ thin films fabricated by spin-coating using a preformed 2D perovskite

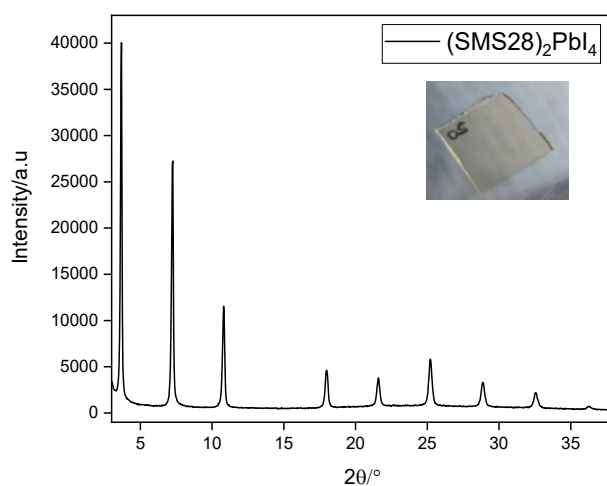


Figure S4. XRPD patterns of the $(\text{SMS28})_2\text{PbI}_4$ thin film obtained by spin coating a 2D perovskite powder dispersion in DMSO.

$(\text{SMS28})_2\text{PbI}_4$ Single Crystals Synthesis.

$(\text{SMS28})_2\text{PbI}_4$ crystals were obtained by mixing in an autoclave a stoichiometric amount of the organic cation **SMS28** and PbI_2 in concentrated HI and then heated at 100°C for 24 h. The autoclave was cooled to room temperature with a rate of $7^\circ\text{C}/\text{h}$ to promote the crystals growth. Very flat single crystals of $(\text{SMS28})_2\text{PbI}_4$ were obtained. Due to the lack of growth in the third dimension, only the arrangement of the inorganic PbI_4^{2-} layers has been solved by single crystal X-ray diffraction, as shown in **Figure S5**. The growth of $(\text{LF8})_2\text{PbI}_4$ single crystals was also attempted in the same way but no suitable crystals for data collection were obtained.

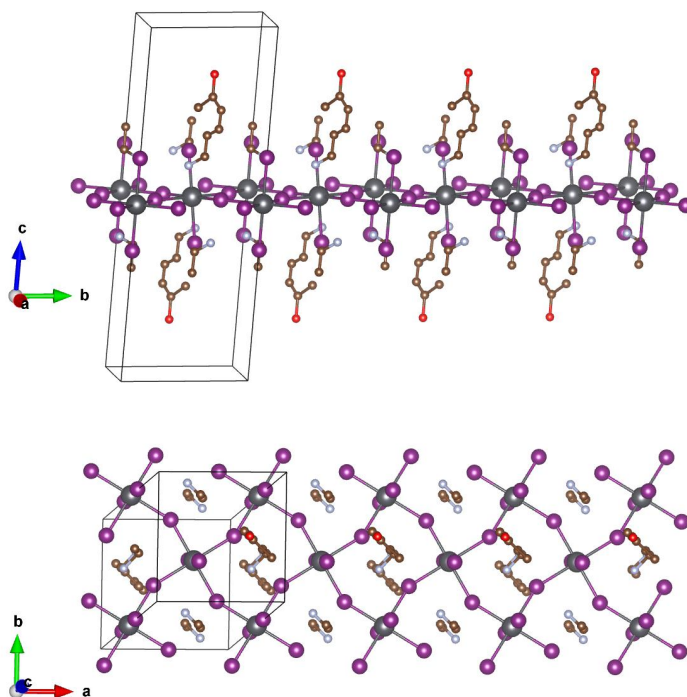


Figure S5. Experimental cell structure obtained from the Single Crystal X-Ray Diffraction of $(\text{SMS28})_2\text{PbI}_4$.

DFT simulations of $(\text{SMS28})_2\text{PbI}_4$ structure

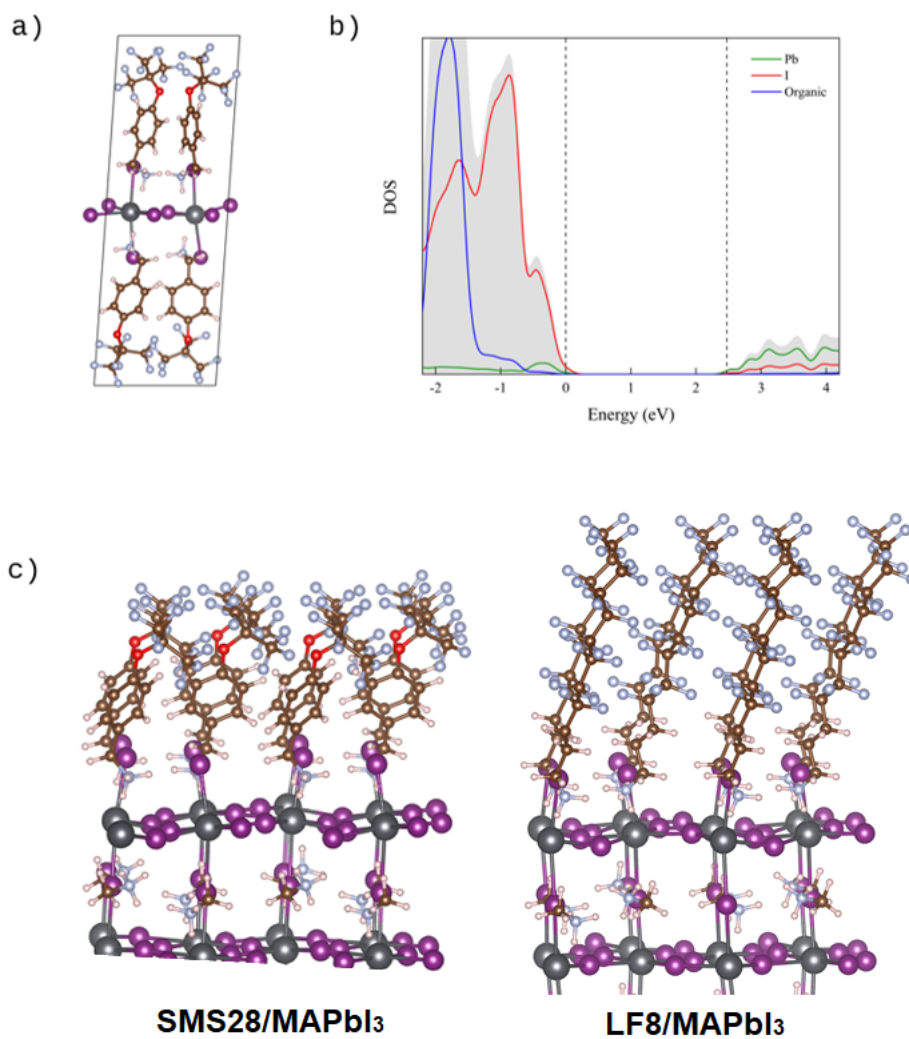


Figure S6. a) Theoretical cell structure obtained from DFT geometrical optimization of $(\text{SMS28})_2\text{PbI}_4$, view along the “c” axis; b) analysis of the electronic properties by DFT Density of States analysis (DOS) of $(\text{SMS28})_2\text{PbI}_4$; c) simulation of the interface between MAPbI₃ and an interacting SMS28 or LF8 passivating layer.



Figure S7. Relative Humidity control setup and measurement verification.

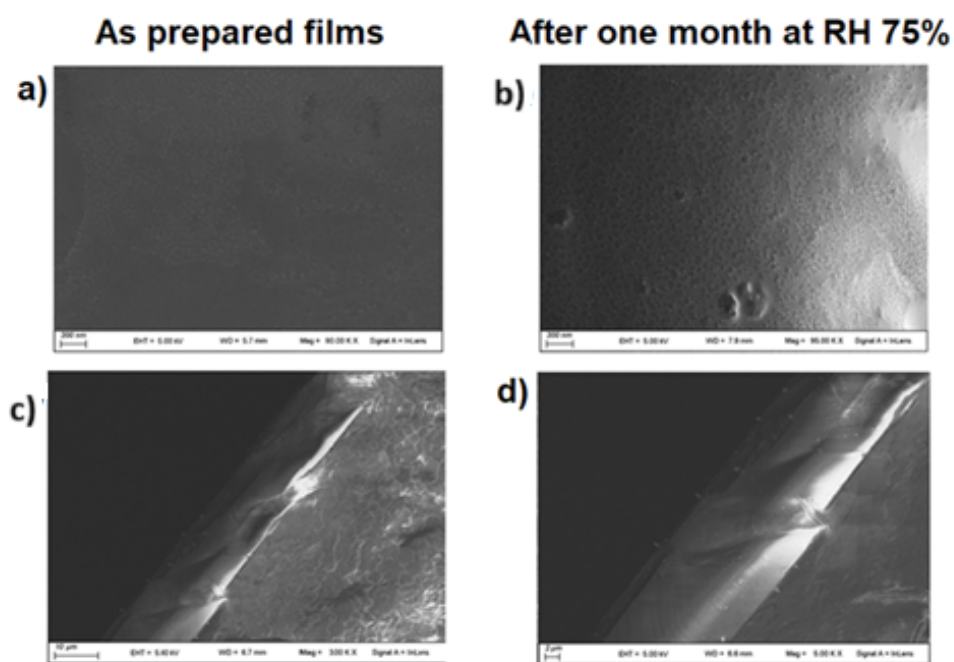


Figure S8. Humidity resistance tests (RH 75%) of $(\text{LF8})_2\text{PbI}_4$ thin films. Lateral (**Figure S8a** and **Figure S8b**) and cross-sectional (**Figure S8c** and **Figure S8d**) SEM images of thin films before and after one-month exposure to RH 75%.

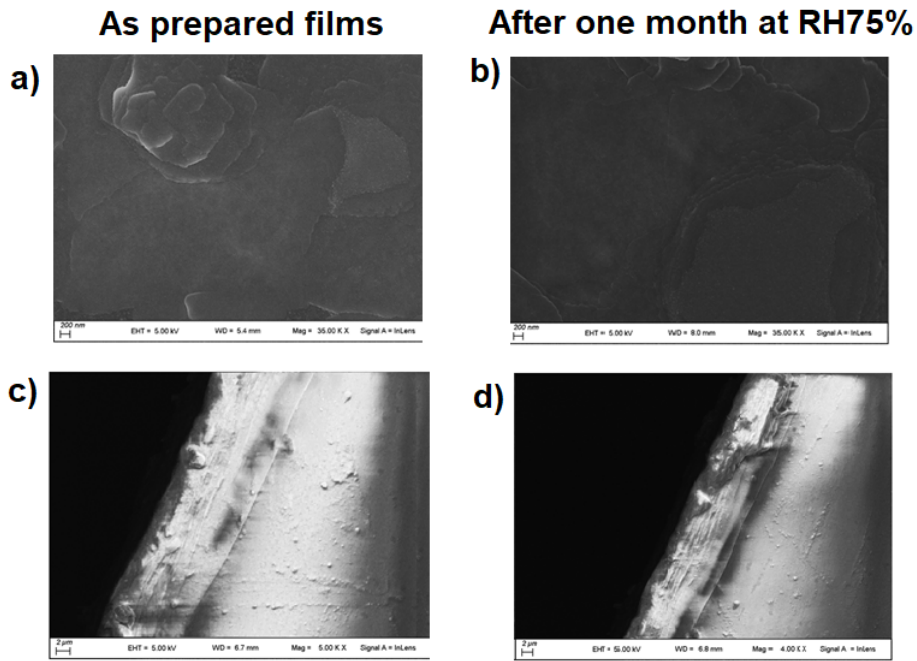


Figure S9. Humidity resistance tests (RH 75%) of $(\text{SMS28})_2\text{PbI}_4$ thin films. Lateral (Figure S9a and Figure S9b) and cross-sectional (Figure S9c and Figure S9d) SEM images before and after one-month exposure to RH 75%.

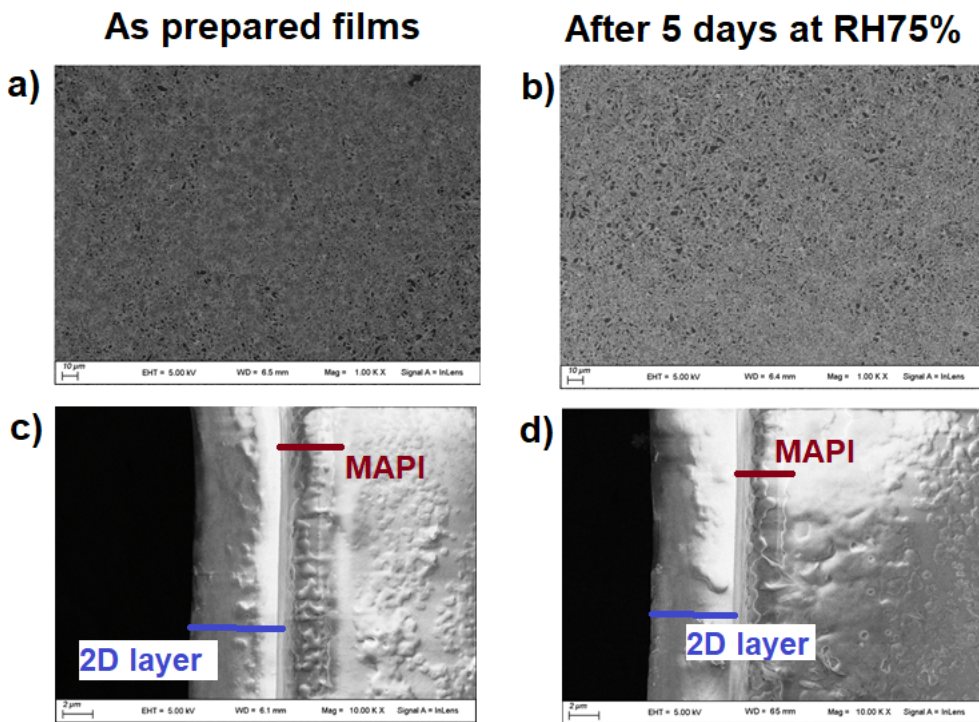


Figure S10. Humidity resistance tests (RH 75%) of $(\text{LF8})_2\text{PbI}_4/\text{MAPbI}_3$ heterojunction films. Lateral (Figure S10a and Figure S10b) and cross-sectional (Figure S10c and Figure S10d) SEM images before and after one-month exposure to RH 75%.

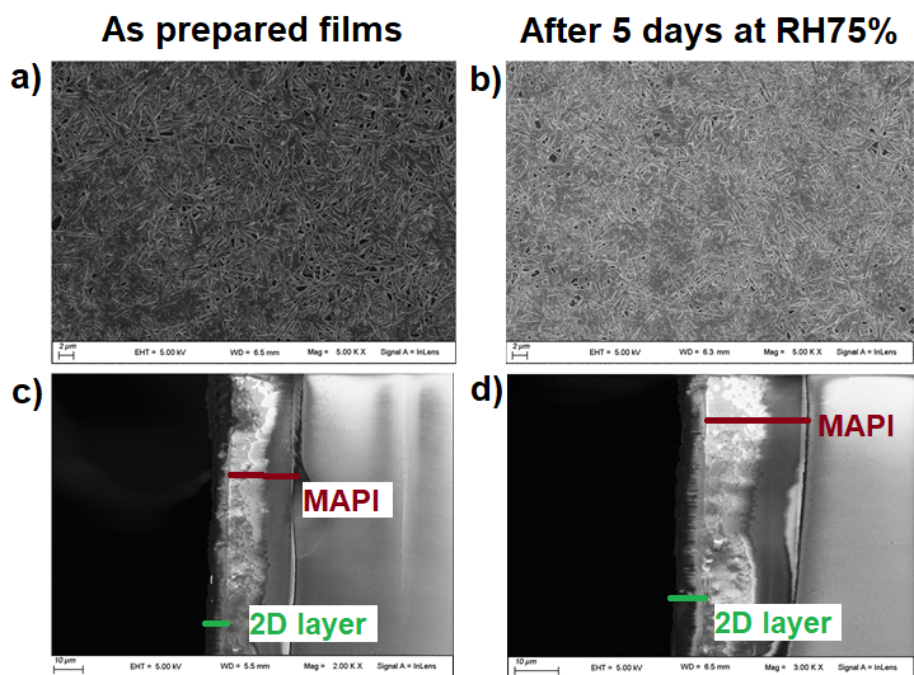


Figure S11. Humidity resistance tests (RH 75%) of $(\text{SMS28})_2\text{PbI}_4/\text{MAPbI}_3$ heterojunction films. Lateral (**Figure S11a** and **Figure S11b**) and cross-sectional (**Figure S11c** and **Figure S11d**) SEM images before and after five-days exposure to RH 75%.

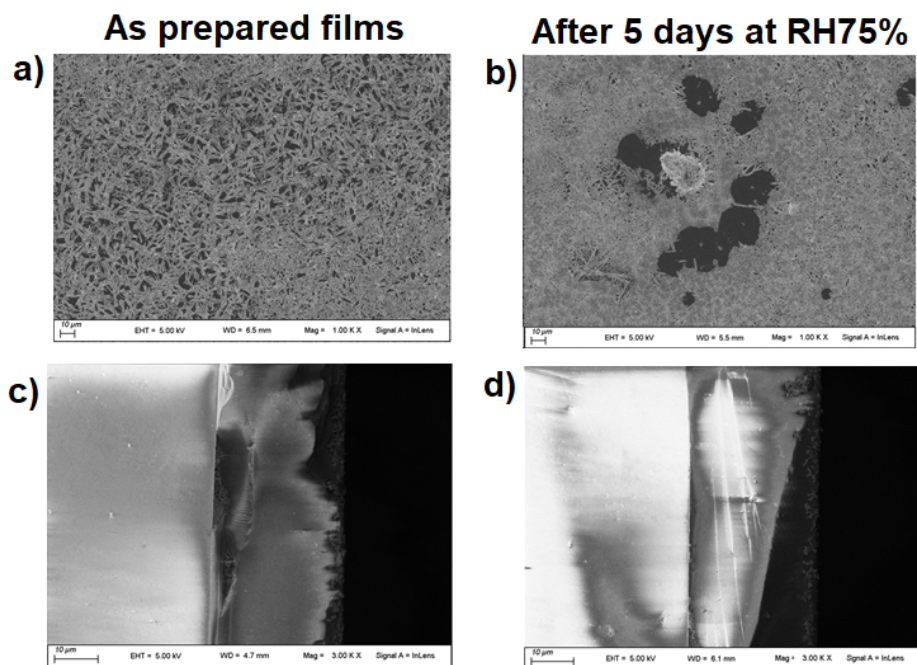


Figure S12. Humidity resistance tests (RH 75%) of MAPbI_3 films. Lateral (**Figure S12a** and **Figure S12b**) and cross-sectional (**Figure S12c** and **Figure S12d**) SEM images before and after five-days exposure to RH 75%.

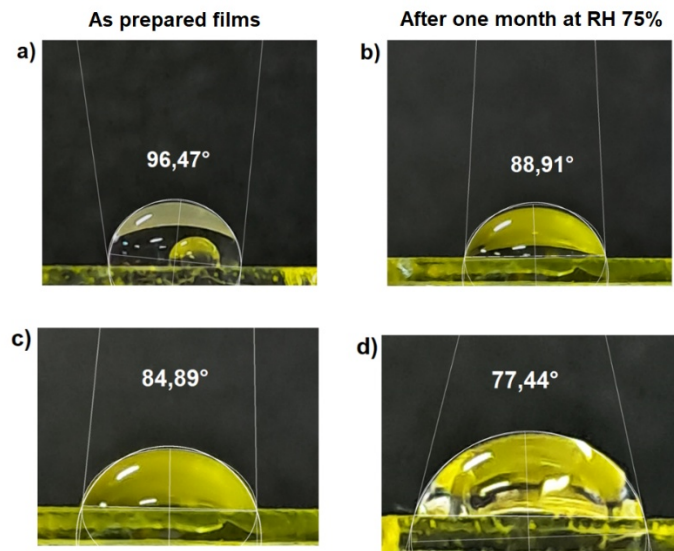


Figure S13. Static water contact angle measurements for $(\text{LF8})_2\text{PbI}_4$ (Figure S13a and Figure S13b) and for $(\text{SMS28})_2\text{PbI}_4$ (Figure S13c and Figure S13d) before and after one-month exposure to RH 75%.

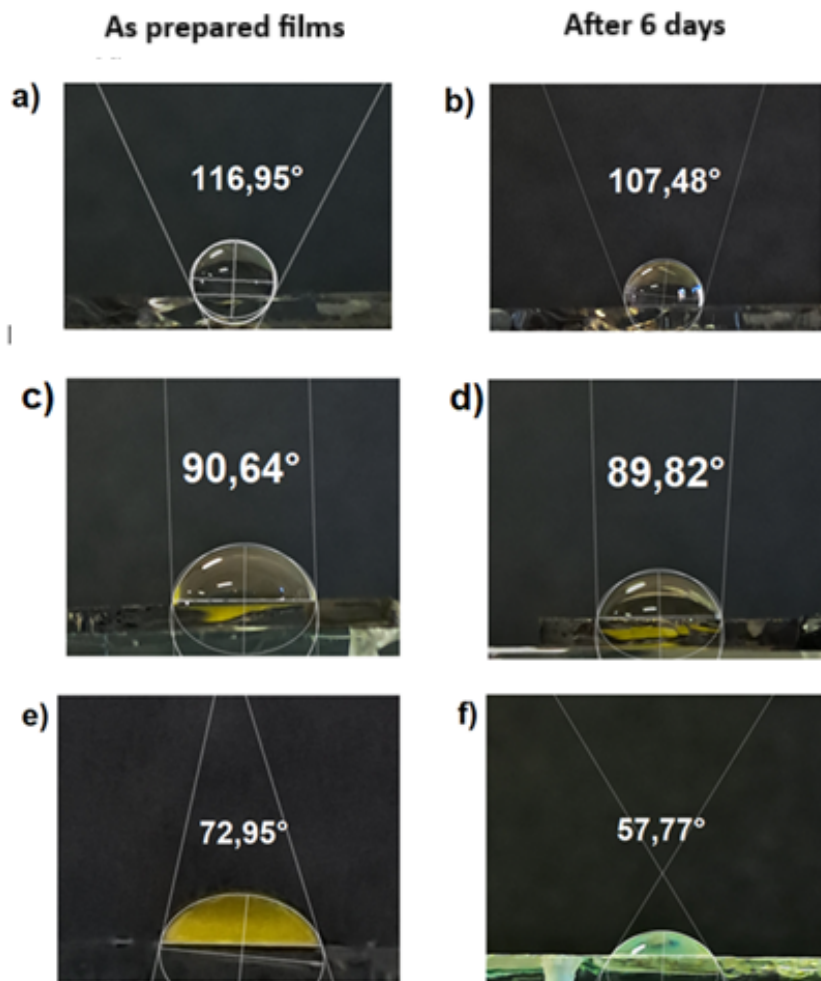


Figure S14. Static water contact angle measurements for $(\text{LF8})_2\text{PbI}_4/\text{MAPbI}_3$ (Figure S14a and Figure S14b), $(\text{SMS28})_2/\text{MAPbI}_3$ (Figure S14c and Figure S14d), and MAPbI_3 (Figure S14e and Figure S14f) before and after 6 days exposure to RH 75%.

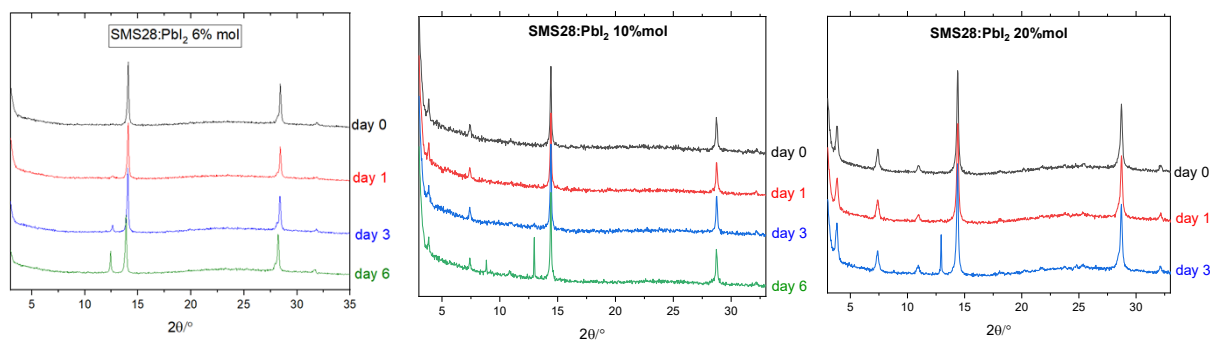


Figure S15. Humidity resistance tests (RH 75%) of the **SMS28-MAPbI₃** “quasi-3D” perovskite. Evolution of XRPD pattern.

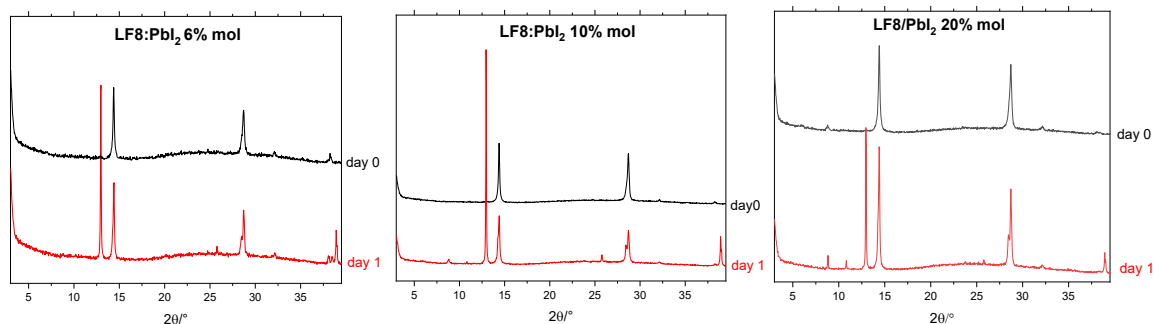


Figure S16. Humidity resistance tests (RH 75%) of the **LF8-MAPbI₃** “quasi-3D” perovskite. Evolution of XRPD pattern.

References

- 1 A. Abulikemu, G. Halász, A. Csámpai, Á. Gömöröy and J. Rábai, *J. Fluorine Chem.*, 2004, **125**, 1143
- 2 M. Berta, A. Dancsó, A. Nemes, Z. Pathó, D. Szabó, J. Rábai, *J. Fluorine Chem.*, 2017, **196**, 57
- 3 H. Meng, L. Wen, Z. Xu, Y. Li, J. Hao and Y. Zhao, *Org. Lett.*, 2019, **21**, 5206